

On the Functionalization of C₆₀ with Vinylallenes Generated *in situ* by Rhodium Catalysis

Cristina Castanyer,^a Albert Artigas,^a Miquel Solà,^a Anna Pla-Quintana,^{a,*} and Anna Roglans^{a,*}

^a Institut de Química Computacional i Catàlisi (IQCC) and Departament de Química, Facultat de Ciències, Universitat de Girona (UdG), C/ Maria Aurèlia Capmany, 69, 17003-Girona, Catalunya, Spain
E-mail: anna.plaq@udg.edu; anna.roglans@udg.edu

Manuscript received: September 16, 2024; Revised manuscript received: October 2, 2024;

Version of record online: ■■, ■■■

Supporting information for this article is available on the WWW under <https://doi.org/10.1002/adsc.202401163>

© 2024 The Author(s). Advanced Synthesis & Catalysis published by Wiley-VCH GmbH. This is an open access article under the terms of the Creative Commons Attribution Non-Commercial NoDerivs License, which permits use and distribution in any medium, provided the original work is properly cited, the use is non-commercial and no modifications or adaptations are made.

Abstract: The functionalization of fullerenes is important for several reasons, primarily related to enhancing their chemical reactivity, solubility, and potential of applications in optoelectronics and biomedicine. In this study, we present a novel approach to functionalize C₆₀ through a cascade process encompassing an unprecedented Rh-catalyzed cycloisomerization of 1,6-allenynes to *in situ* generate a vinylallene that is followed by a Diels-Alder reaction with pristine fullerene, resulting in the formation of 6,6-fused bicyclic fullerene derivatives. The mechanism governing this process was elucidated by DFT calculations and confirmed by deuterium labelling and control experiments, demonstrating the critical role of traces of water in the reaction medium to mediate the observed reactivity.

Keywords: Cycloisomerization; Diels-Alder reaction; Fullerene; Proton transfer; Vinylallene

Introduction

The process of functionalizing pristine C₆₀ with specific chemical groups or by altering its structure enables the customization of fullerene properties to suit diverse needs. Through functionalization, fullerenes can be tailored to exhibit enhanced solubility, improved electronic properties, and to be compatible with a variety of matrices and materials. This process opens up a vast array of possibilities across numerous disciplines including biomedicine,^[1] materials science,^[2] and next-generation photovoltaics.^[3]

It is well established that in C₆₀ the [6,6] bonds, which are shorter and exhibit a double-bond character, actively participate in numerous chemical reactions in which cycloadditions play a pivotal role.^[4,5] Among these, the Diels-Alder (DA) reaction particularly stands out as one of the most versatile transformations.^[6] Indeed, the reaction of fullerenes with dienes has been widely used to decorate the fullerene cage and prepare

novel compounds with unconventional electronic and optical properties. Conversely, vinylallenes have never been described to react with fullerenes.

The substitution of one of the double bonds in the prototypical diene with an allene promotes DA cycloaddition reactions with lower activation barriers and higher exothermicities, unique aspects of diastereoselection, and provides cycloadducts with an exocyclic C=C bond in conjugation with the usual cyclohexene one.^[7] However, transformations that grant access to allenes in general and vinylallenes in particular, although they have been better developed recently,^[8] are not as straightforward as those that produce dienes.

In contrast to the numerous examples of DA reactions in fullerenes, there are few cases where the diene is generated *in situ*, resulting in a highly versatile cascade process. Transition-metal catalyzed cycloisomerizations of unsaturated substrates^[9] are an efficient method for the *in situ* generation of exocyclic dienes. In this line, we have recently described tandem Rh-

catalyzed cycloisomerization of 1,6-enynes^[10] and 1,5-bisallenyls^[11] to *in situ* generate a diene that subsequently reacted by a DA reaction with C₆₀ (Scheme 1a). This resulted in the formation of 6,5- and 6,7-fused C₆₀ bicyclic systems, respectively. Mechanistically, DFT calculations demonstrated that the rhodium metal coordinates to the two unsaturations to then form the corresponding metallacycle intermediate. For the 1,6-enynes and using [Rh(cod)₂]BF₄/(R)-Tol-BINAP as

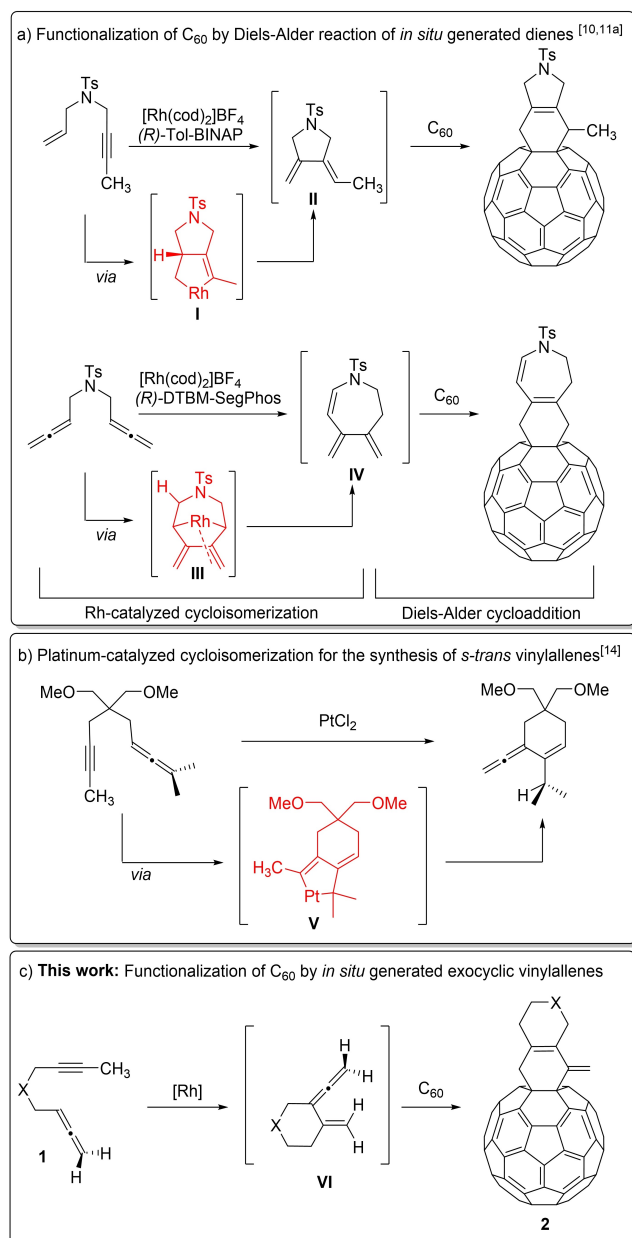
a catalytic system, rhodacyclopentene complex **I** is generated, which evolves into exocyclic cyclopentane-1,3-diene **II**. For the 1,5-bisallenyls^[11a] the oxidative coupling took place at the central carbon atoms of both allene moieties to deliver rhodabicyclo[3.2.1]octane intermediate (**III**) that then evolved to cycloheptene-1,3-diene **IV** under Rh catalytic system ([Rh(cod)₂]BF₄/(R)-DTBM-SegPhos).

Whereas cycloisomerization reactions leading to exocyclic dienes have been widely explored, to the best of our knowledge, only one example has reported the generation of vinylallenes through transition-metal catalyzed cycloisomerization. Whilst 1,6-allenynes were initially reported to afford six-membered triene carbocycles under cobalt-catalysis^[12] and later described to afford a wide variety of carbocycles and heterocycles, with different sizes and structures with other metals,^[9i,13] Malacria et al.^[14] described in 2004 that platinum catalysis facilitated the isomerization of 1,6-allenynes with a methyl group at the terminus of the alkyne (Scheme 1b) to generate an *s-trans* vinylallene.

In this process, the initially formed platinumacyclopentene intermediate **V** underwent regioselective β-H elimination from the allylic methyl group rather than the *gem*-methyl hydrogen atom, resulting in the production of a vinylallene derivative. The complete mechanistic pathway and specifically the regioselective preference for the β-H elimination from the methyl group in the allylic position of intermediate **V** was theoretically studied and demonstrated by Soriano et al.^[15]

Since the selectivity of the cycloisomerization reactions can be widely modulated by tuning the catalytic system and the reaction medium, we wondered whether by starting with 1,6-allenynes with a methyl at the terminus of the triple bond it would be feasible to generate an exocyclic vinylallene **VI**, that differs from the vinylallene observed in the platinum catalysis scenario in that **VI** is exocyclic and thus fixed in the *s-cis* conformation. Such an *in situ* generated vinylallene **VI** might subsequently undergo a DA cycloaddition with pristine fullerene, resulting in the formation of 6,6-fused C₆₀ derivatives (Scheme 1c).

Here we describe our findings concerning the cascade process based on an unprecedented cycloisomerization of 1,6-allenynes **1** in the presence of a rhodium catalyst to afford a vinylallene that reacts through a DA reaction with pristine fullerene. Moreover, a complete mechanistic study of this transformation has been undertaken by DFT calculations and control and deuterium labelling experiments unravelling the key role of water present in the reaction medium. Through this cascade process, we aim to expand the spectrum of ring fusions with fullerene, specifically targeting the formation of 6,6-fused deriv-



Scheme 1. a) Methods for the functionalization of C₆₀ via a Diels-Alder reaction with *in situ* generation of dienes through cycloisomerization reactions, b) single precedent on the cycloisomerization of 1,6-allenynes for the generation of *s-trans* vinylallenes and c) the functionalization of C₆₀ with *in situ* generated vinylallenes presented herein.

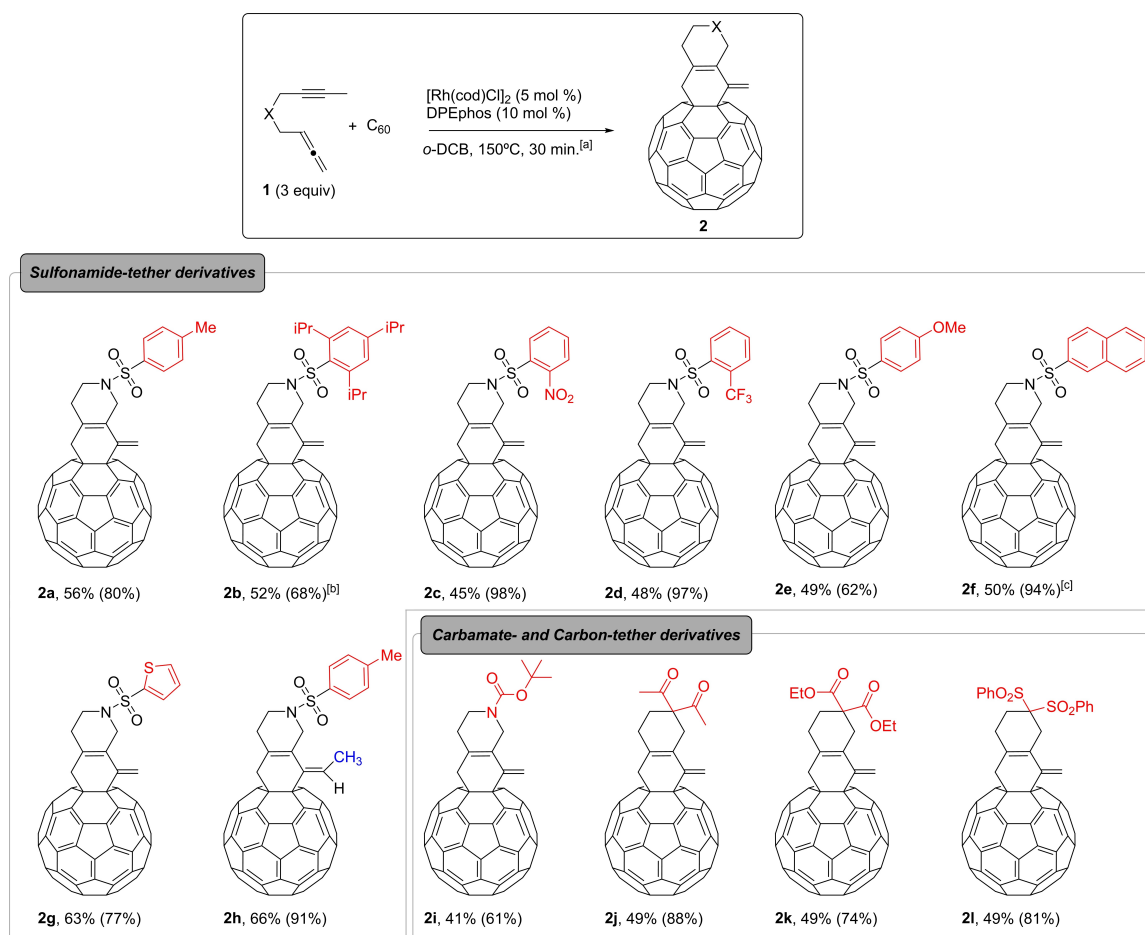
atives that were not achieved in our previous cases (Scheme 1a).

Results and Discussion

The study commenced by testing the reaction conditions for the cycloaddition between *N*-tosyl-tethered allenyne **1a** and fullerene C₆₀ (Scheme 2). Inspired by the work of Breit et al.^[16] that reported the cycloisomerization of 1,6-allenenes to afford six-membered exocyclic 1,3-diene by using [Rh(cod)Cl]₂ (cod = cyclooctadiene) and bis[(2-diphenylphosphino)ether] (DPEphos) as a catalytic system, we initially employed such a mixture of rhodium complex [Rh(cod)Cl]₂ and DPEphos, which was pre-treated under hydrogenation conditions. After some experimentation (see Table S1 in the Supporting Information), the best reaction conditions were found to be 3 equivalents of allenyne **1a** at a concentration of [C₆₀] = 1.4 M in *o*-dichlorobenzene (*o*-DCB) at 150 °C for 30 minutes. As a

result, product **2a** was obtained with a yield of 56%. Further efforts to optimize the reaction conditions involved varying the ligand. However, when other biaryl biphosphines (BIPHEP, (*R*)-DTBM-Segphos, Xantphos, (*R*)-H₈-BINAP, (*R*)-Tol-BINAP) were used the performance of the reaction was significantly worse. An additional attempt using the cationic [Rh(cod)₂]BF₄ with DPEphos gave only a 5% yield of **2a**. Finally, two blank experiments were performed, demonstrating that the presence of both Rh and the ligand was imperative to the success of the process.

With an optimized set of conditions at hand, the scope of the reaction was then examined (Scheme 2). With sulfonamide tethered allenyne **1a–1h**, the corresponding fullerene derivatives **2a–2h** were obtained with yields up to 66%. Alkyl (**2a**, **2b**), electron-withdrawing (**2c**, **2d**), and electron-donating groups (**2e**) in the phenylsulfonamide as well as naphthalene (**2f**) and thiophene (**2g**) sulfonamides were tolerated in the process and fullerene derivatives **2a–2g** were

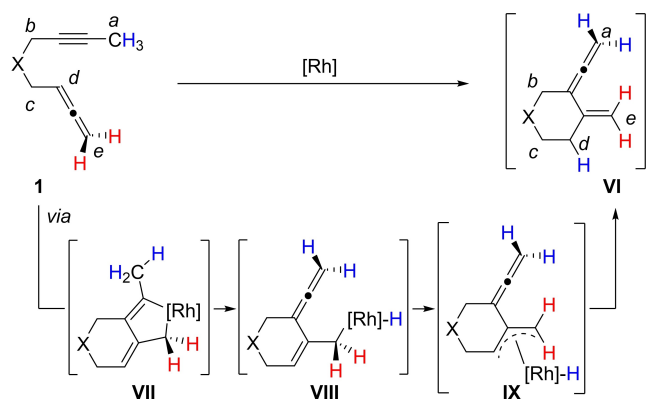


Scheme 2. Scope of the cycloaddition of allenyne **1** with C₆₀. The yields in parentheses are based on the amount of C₆₀ consumed. ^[a]Unless otherwise noted the reactions were performed with C₆₀ (0.07 mmol), **1** (0.22 mmol), [Rh(cod)Cl]₂ (5 mol%), DPEphos (10 mol%), *o*-DCB (50 mL), 150 °C, 30 min (TLC monitoring). ^[b]The reaction was run for 45 min. ^[c]The reaction was run for 20 min.

obtained with good yields. An allenyne **1h** with an ethyl group at the alkyne terminus successfully underwent the reaction, resulting in the diastereoselective formation of (*E*) derivative **2h** with a 66% yield. With regard to the tether, not only sulfonamides but also *tert*-butylcarbamate (**1i**), 1,3-diketone (**1j**), malonate (**1k**), and bisphenylsulfonyl (**1l**) allenyne reacted with fullerene, giving compounds **2i–2l**, respectively, with good yields.

In order to thoroughly investigate the mechanism of this new process, deuterium labelling experiments were performed together with DFT calculations. According to our mechanistic hypothesis (Scheme 3), oxidative coupling between the alkyne and the external double bond of the allene would lead to rhodabicyclic intermediate **VII**, which then may eventually generate vinyl allene intermediate **VI** via a Rh-assisted proton transfer taking place between *Ca* and *Cd*, passing through intermediates **VIII** and **IX**. Finally, intermediate **VI** would react in a Diels-Alder cycloaddition reaction with C_{60} delivering cycloadduct **2**.

The occurrence of polyadducts in DA reactions involving fullerenes has been well-documented.^[6] Most notably, the Rh-catalyzed reaction of C_{60} with bisallenes, which has been established as proceeding through the cycloisomerization/[4+2] pathway,^[11] results in the formation of bisadducts when an excess of bisallene is present in the reaction mixture. Following this idea, we reasoned that if the reaction mechanism that leads to cycloadducts **2** involves a [4+2] cycloaddition with **VI**, the presence of 3 equiv. (Scheme 2) in the reaction mixture would result in polyaddition at some extent. To test this, we run the reaction of C_{60} with allenyne **1a**, but this time allowing the reaction to stir for additional 60 minutes, at which time a retained spot was clearly observed by TLC monitoring. Isolation of this fraction with 100% CH_2Cl_2 , and subsequent analysis by MALDI-MS revealed peaks corresponding to the bis and tris adducts (see Supporting Information). Moreover, during the reaction with



Scheme 3. Mechanistic hypothesis for the formation of vinylallene intermediate **VI**.

the 1,6-allenyne **1d**, the same spot was observed after 30 min. The fraction was isolated, revealing again the presence of polyadducts by MALDI-MS. This result represents an indirect proof of the formation of intermediate **VI** during the process. Unfortunately, intermediate **VI** could not be isolated when conducting the reaction in the absence of C_{60} . Conversely a complex mixture of unidentified products was obtained, suggesting that **VI** is indeed an unstable and very reactive species.

With the aim to confirm the importance of the methyl protons in the proton transfer taking place during the cycloisomerization mechanism, we opted to conduct additional tests involving phenyl-substituted 1,6-allenyne **1m**, and deuterated **1aa** and **1ab** (Figure 1). As expected, **1m** does not react with C_{60} , as no protons can be abstracted from *Ca*. In turn, product **3m** was isolated in a 37% yield from an intramolecular [2+2] cycloaddition of **1m**, involving the triple bond and the external double bond of the allene (Figure 1a). The cycloaddition under standard reaction conditions was then performed with allenyne **1aa**, containing two

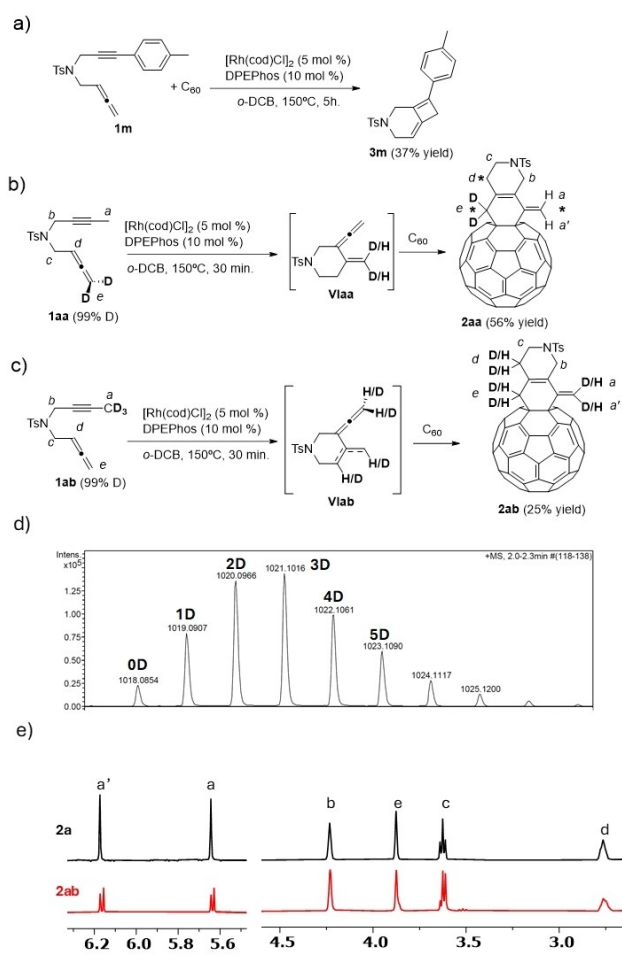


Figure 1. Control and deuterium experiments. Minor scrambling in **2aa** indicated with asterisks.

deuterium atoms at the terminal allene position *e*. Cycloadduct **2aa** was isolated upon reaction with C₆₀ (Figure 1b). The deuterium atoms are located almost exclusively at the methylene group directly connected to the fullerene cage. However, minor scrambling into positions *a* and *d* was detected by ¹H NMR spectra, and the loss of one of the deuterium atoms was observed in small proportion, as ascertained by the observation of a small peak in the HRMS corresponding to [C₇₅H₁₆DNSO₂+Na]⁺ species (vide infra for the justification of the observations).

By its part, allenyne **1ab** containing a deuterium methyl group at *Ca* provides **2ab** after reaction with C₆₀. In this latter case, the deuterium atoms appear at the expected position *a* and *d*, but also at position *e*. Moreover, proton signals were observed in all positions, including *Ca*. ESI-HRMS and ¹H-NMR spectroscopy were used to determine the number and positions of the deuterium atoms in **2ab** (Figure 1d and e). The mass spectra revealed the presence of up to five deuterated species as sodium adducts, and also the protio substrate at *m/z* = 1018.0854 (Figure 1d). Comparing the NMR spectra of compound **2a** with that of compound **2ab** (Figure 1e) the two olefinic protons in **2ab** appear as four singlets, corresponding to the three combinations H/H, H/D, D/H at position *a* (i.e. the chemical shift of the proton signal is slightly shifted by the presence of a deuterium in the geminal position).

The integration of protons at position *d* at δ = 2.76 ppm is less than 2, indicating that some deuterium exchanged with protons in this position. In addition, the two protons at position *c* observed at δ = 3.61 ppm change in multiplicity from a triplet to a doublet, although a residual triplet is also observed overlapped with the doublet.

The results obtained with the labelled allenyne indicate that several proton transfer processes occur during the reaction. To better understand this, the mechanism illustrated in Scheme 3 was simulated via a DFT study performed at the M06L–D3/cc-pVTZ-PP(SMD = *o*-DCB)//B3LYP–D3/cc-pVDZ-PP level of theory at 423.15 K (Figure 2).^[17] The calculations revealed a considerably high barrier of 35.5 kcal/mol estimated for the proton abstraction step from intermediate **VII** to **VIII**. Together, the experimental data and computations suggest that the formation of **VI** from **1a** may occur through an alternative more complex reaction mechanism than that depicted in Scheme 3. Inspired by a recent study on the Rh^I-catalyzed cycloisomerization reaction of enevinylidenecyclopropanes,^[18] as well as previous results from the group on the thermal cycloisomerization of macrocyclic triynes and enediynes involving formation of a vinylallene,^[19] in which the presence of water was found to be key to explaining a proton transfer process, we decided to test this possibility through additional

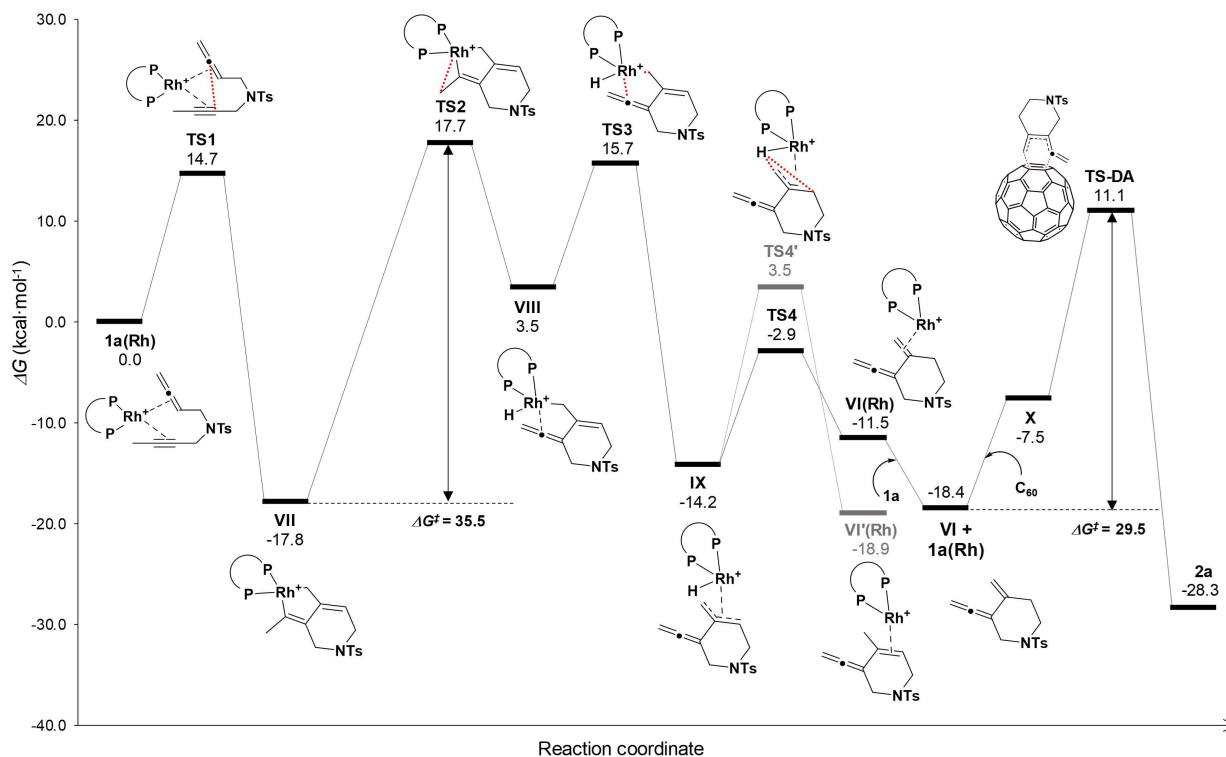


Figure 2. M06L–D3/cc-pVTZ-PP(SMD = *o*-DCB)//B3LYP–D3/cc-pVDZ-PP Gibbs energy profile ($T=423.15$ K) of the Rh-catalyzed cascade cycloisomerization/[4 + 2] cycloaddition of **1a** and C₆₀.

experiments. Two reactions were conducted with **1a** under optimal reaction conditions. The first trial was performed in completely anhydrous conditions using anhydrous *o*-DCB and 4 Å molecular sieves in the Schlenk flask. Under these conditions, the reaction failed, and the C_{60} was recovered quantitatively. This result indicates that, trace amounts of water are essential for the reaction to succeed. To elucidate whether H_2O can act as an external proton source, a second experiment was conducted. Accordingly, two drops of D_2O were added to the reaction mixture. The corresponding cycloadduct was obtained this time in a 18% yield. Interestingly, the HRMS spectrum corroborated the incorporation of up to five deuterium atoms into the final product (Figure 3a), and the 1H NMR spectrum closely matched that of deuterated **2ab** (Figure 3b). In addition, deuterium NMR spectra showed broad signals at $\delta=2.7$ and 5.6–6.1 ppm corresponding to the *d* and *a* position, respectively, together with a minor peak at $\delta=3.8$ ppm corresponding to the *e* position (see Supporting Information). A third experiment was then performed starting with

deuterated **1ab** adding two drops of D_2O to the reaction medium. In this case, unlabelled **2ab** was not observed in HRMS (Figure 3a) and only residual signals of the olefinic protons *a* were observed in the 1H NMR spectrum (Figure 3b). In addition, deuterium NMR of **2ab** shows three broad signals at $\delta=2.7, 3.8, 5.6$ – 6.1 ppm corresponding to deuterium atoms in positions *d, e* and *a/a'*, respectively. This confirms the D–H exchange during the reaction and highlights the critical role of trace amounts of water acting as a proton source in the reaction (see experimental details in the Supporting Information).

Once the involvement of water was demonstrated experimentally, we performed additional DFT calculations to investigate the precise reaction mechanism that leads from allenyne **1a** to intermediate **VI**. Diverse reaction pathways involving the intervention of 1, 2 or 3 water molecules were considered in the reaction model. Figure 4 represents the lowest in energy computed Gibbs energy profile (see Supporting Information for the other possibilities). After much investigation, we concluded that the reaction starts by coordination of the Rh-biphosphine complex to allenyne **1a**, thus forming square planar 16-electron species **1a(Rh)**. The Rh^I centre is found η^2 -coordinated to the triple bond and the internal double bond of the allene moiety in this intermediate. Oxidative coupling at **1a(Rh)** through **TS1** ($\Delta G^\ddagger = 14.7$ kcal mol $^{-1}$) results in square pyramidal 5–6 fused rhodacyclopentene intermediate **VII**, which is found 17.8 kcal mol $^{-1}$ lower in the Gibbs energy surface. Subsequently, two molecules of water coordinate to the Rh^{III} centre to generate octahedral 18-electron intermediate, **XI-aq**, in a process that releases 2.8 kcal mol $^{-1}$. Water coordination in **1a(Rh)** prior to the oxidative coupling step was also considered, but the corresponding **TS1-aq** was found to be much higher in energy ($\Delta G^\ddagger = 36.6$ kcal mol $^{-1}$). Next, one of the water molecules delivers one proton to *Cd*. This process has a cost of 28.4 kcal mol $^{-1}$ through **TS2-aq** and is endergonic by 10.8 kcal mol $^{-1}$. The result of this first proton transfer is hydroxo Rh^{III} complex **XII-aq**, which is in equilibrium with isoenergetic **XIII-aq** through a very low barrier of 3.4 kcal mol $^{-1}$ (**TS3-aq**). The oxidation state of similar reaction intermediates raised controversy,^[20] thus the oxidation state of intermediate **XII-aq** has been analysed and determined to be +3 by effective oxidation states (EOS) analysis.^[21] From **XIII-aq**, abstraction of one proton from the methyl group to a hydroxo ligand via **TS4-aq** ($\Delta G^\ddagger = 13.4$ kcal mol $^{-1}$) regenerates the water molecule and completes the formal proton transfer from *Ca* to *Cd*, giving **XIV-aq**. Proton delivery at *Ce* was also computed, but this reaction path was discarded as the corresponding transition state **TS2'-aq** was found to be 11.3 kcal mol $^{-1}$ higher. Satisfyingly, the inclusion of two water molecules in the reaction model reduces the

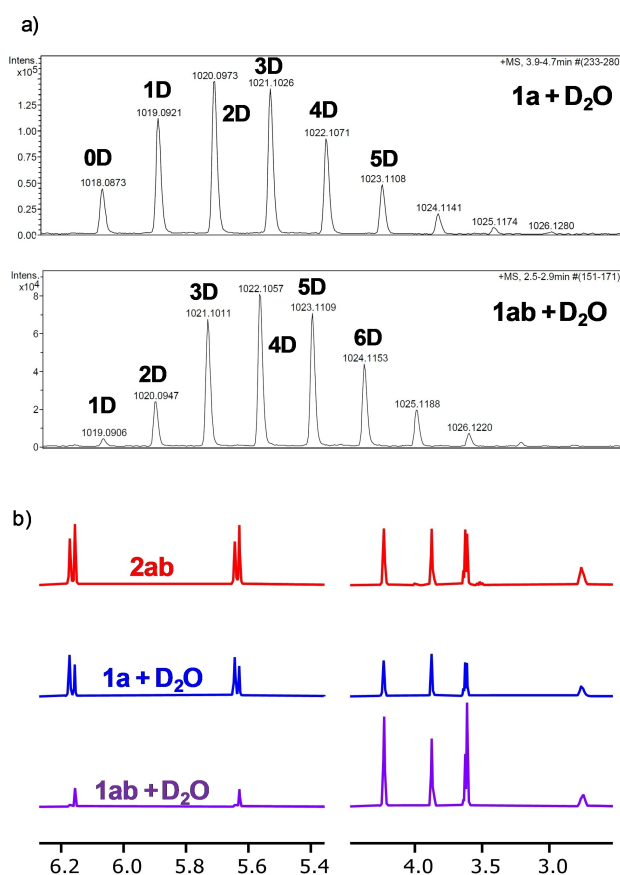


Figure 3. a) ESI-HRMS of the product obtained from **1a** adding 2 drops of D_2O and ESI-HRMS of the product obtained from **1ab** and two drops of D_2O ; b) 1H -NMR spectra of **2ab**, of product obtained from **1a** with two drops of D_2O , and of product obtained from **1ab** with two drops of D_2O .

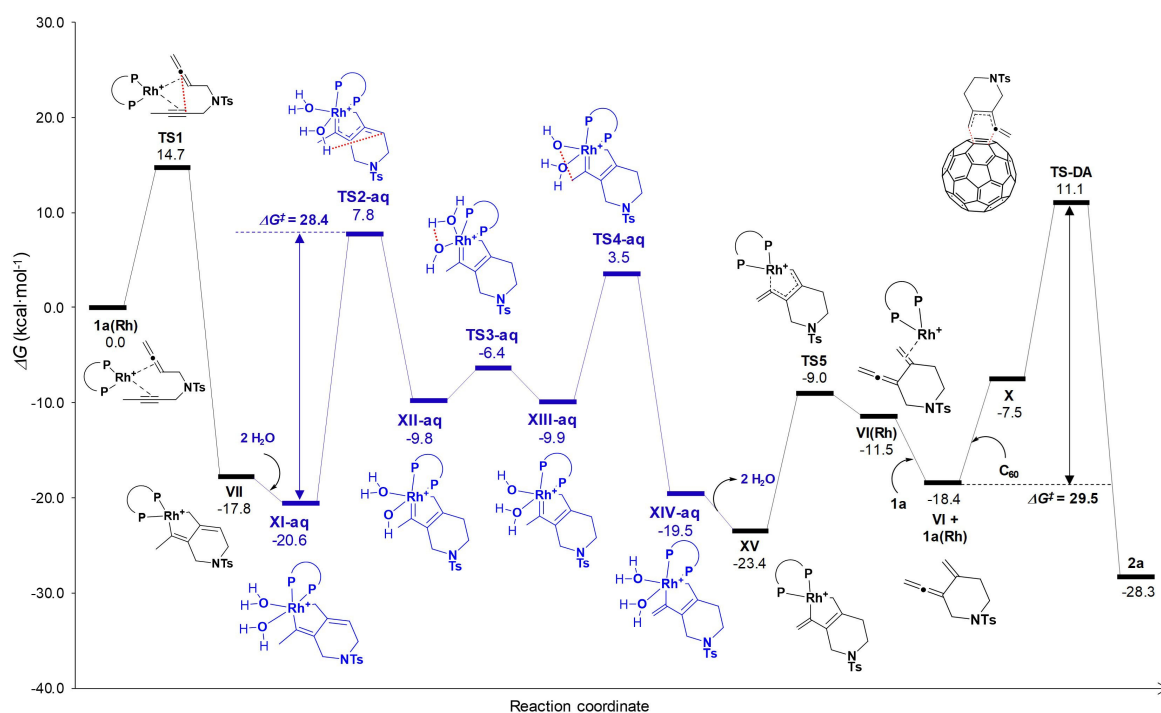


Figure 4. M06L–D3/cc-pVTZ-PP(SMD = *o*-DCB)//B3LYP–D3/cc-pVDZ-PP Gibbs energy profile ($T=423.15$ K) of the Rh-catalyzed cascade cycloisomerization/[4 + 2] cycloaddition of **1 a** and C_{60} including two water molecules in the reaction model.

energy barrier associated with the proton transfer step by $7.1 \text{ kcal mol}^{-1}$, making the reaction feasible under the experimental conditions employed. Decoordination of the two water molecules from **XIV-aq** yields **XV**, which eventually evolves into **VI** by reductive elimination, liberation of the catalyst, and the entrance of a new molecule of **1 a**. This reductive elimination step has an associated energy barrier of $14.4 \text{ kcal mol}^{-1}$ and is endergonic by $5.0 \text{ kcal mol}^{-1}$. Finally, as **VI** forms, it is readily consumed by reacting with C_{60} in a [4 + 2] cycloaddition ($\Delta G^\ddagger = 29.5 \text{ kcal mol}^{-1}$), thus delivering final product **2 a** and allowing the catalytic cycle to proceed despite the endergonic nature of the last steps.

A closer look into the whole reaction mechanism as described in Scheme 4 allowed us to rationalize the occurrence of the complex scenario presented in Figures 1 and 3. First, the detection of H atoms at position *a/a'* upon reaction of **1 ab** (Figure 1c and e) can be explained by the reversible nature of all reaction steps from **XI-aq** until the release of **VI** (that can exchange the protons in blue in position *a* for protons in green coming from water). This same equilibrium also explains the observation of either protons or deuteriums in position *d* in the same reaction. Second, the proportion of deuterium detected in position *e* of **2 ab** can be explained as a result of an equilibrium between species **VI(Rh)** and **IX**, which is in turn in equilibrium with **VI'(Rh)** (equilibrium that exchanges the green and red protons). In this way, a D atom initially installed in the methyl group in position *a* (in

blue in Scheme 4) could end up in position *e* through a water-mediated reversible transfer to *d* (via **VII** to **VI(Rh)** equilibria) and subsequent transfer to *e* through reversible Rh-assisted proton transfer (via **VI(Rh)** to **VI'(Rh)** equilibrium).

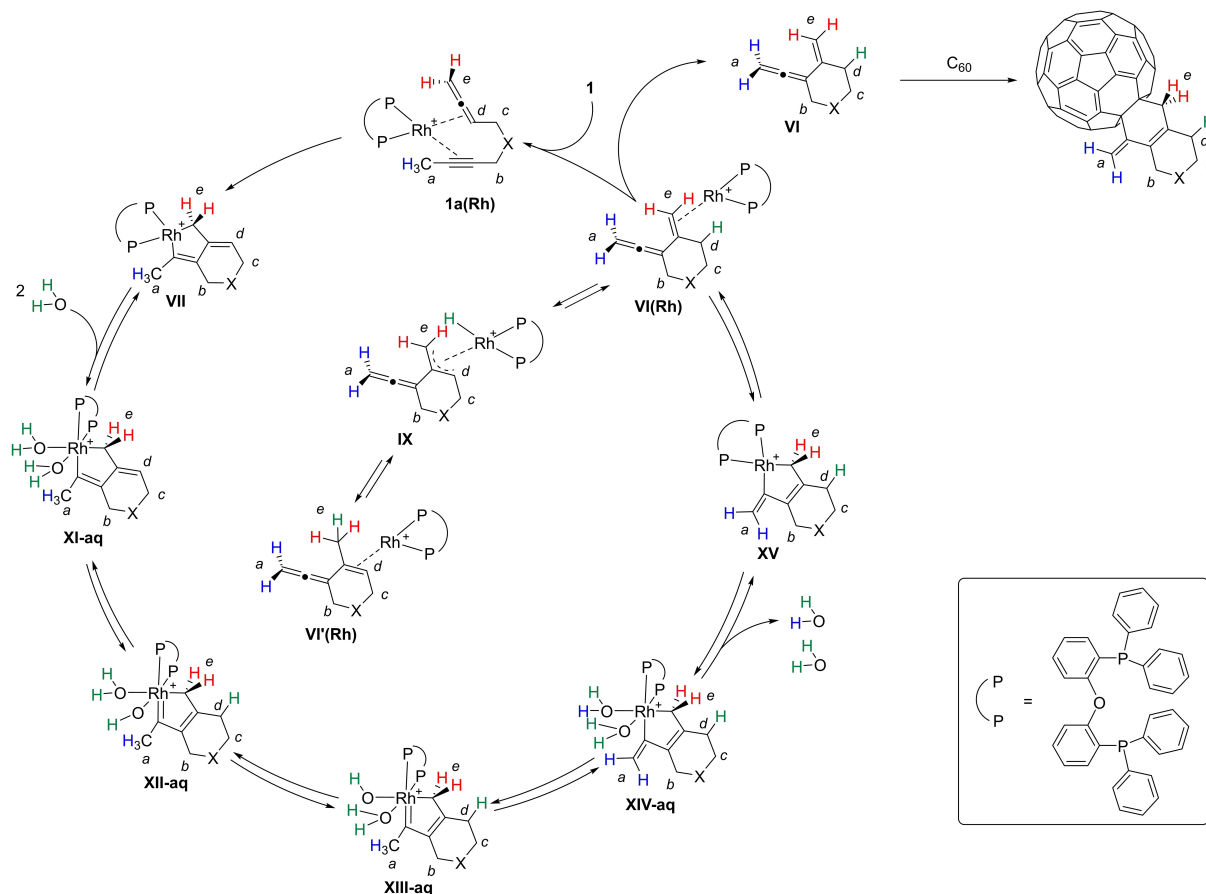
Conclusion

In conclusion, we have unveiled a novel cycloisomerization of allenynes that selectively produces a transient exocyclic vinylallene. This reactive intermediate enables the *in situ* functionalization of C_{60} via an unprecedented vinylallene- C_{60} Diels-Alder cycloaddition. The reaction mechanism has been meticulously investigated through a combination of experimental tests, DFT calculations, and deuterium labelling experiments, revealing that trace amounts of water are crucial for the key regioselective Rh-assisted proton transfer.

Experimental Section

General Procedure for the Synthesis of Derivatives of C_{60} (**2 a**)

In a 10 mL capped vial under a nitrogen inert atmosphere, a solution of $[Rh(\text{cod})Cl]_2$ (1.8 mg, 0.0037 mmol) and DPEphos (4.3 mg, 0.0079 mmol) in anhydrous CH_2Cl_2 (4 mL) was prepared. Hydrogen gas was bubbled into the catalyst solution for 30 min before it was concentrated to dryness, dissolved in anhydrous *o*-DCB and transferred via syringe into a 100 mL



Scheme 4. Mechanism for the water assisted cycloisomerization of allenyne **1** and subsequent Diels-Alder reaction of the *in situ* generated vinylallene **VI** and C_{60} .

Schlenk flask where a solution of C_{60} (51.0 mg, 0.07 mmol, 1 equiv.) and allenyne **1a** (61.0 mg, 0.22 mmol, 3 equiv.) in anhydrous *o*-DCB ($[C_{60}] = 1.4$ mM), is already preheated to 150 °C. The resulting mixture was stirred at 150 °C for 30 min (TLC monitoring). The reaction mixture was purified by column chromatography using CS_2 as the eluent to provide unreacted C_{60} (15.7 mg). Further elution with CS_2 /toluene (1:1) followed by toluene provided compound **2a** as a dark brown solid (39.2 mg, 56% yield, 80% yield based on consumed C_{60}).

Computational Details

Geometries of all stationary points were optimized without symmetry constraints with the Gaussian 16 program^[22] using the DFT B3LYP hybrid exchange-correlation functional^[23] in conjunction with the all-electron cc-pVDZ basis set.^[24] The cc-pVDZ-PP basis set containing an effective core relativistic pseudopotential was used for Rh.^[25] The electronic energy was improved by performing single point energy calculations with the cc-pVTZ-PP basis set and the M06-L functional^[26] and including solvent effects corrections for *o*-DCB computed with the solvent model based on density (SMD).^[27] The D3 Grimme energy corrections for dispersion with the original damping function were added in all B3LYP/cc-pVDZ-PP and M06-L/cc-pVTZ-PP calculations.^[28] Analytical Hessians were computed

to determine the nature of stationary points (one and zero imaginary frequencies for TSs and minima, respectively) and to calculate unscaled zero-point energies (ZPEs) as well as thermal corrections and entropy effects using the standard statistical-mechanics relationships for an ideal gas.^[29] These two latter terms were computed at 423.15 K and 1 atm to provide the reported relative Gibbs energies. As a summary, the reported Gibbs energies contain electronic energies including solvent effects calculated at the M06-L–D3/cc-pVTZ(SMD=*o*-DCB)//B3LYP–D3/cc-pVDZ-PP level together with gas phase thermal and entropic contributions computed at 423.15 K and 1 atm with the B3LYP–D3/cc-pVDZ-PP method. All computational data concerning reaction mechanisms and conformational analyses was uploaded to the ioChem-BD repository^[30] and is available through the following link: <https://iochem.udg.edu/browse/handle/100/6211>.

Acknowledgements

We are grateful for financial support from the Spanish Ministerio de Ciencia, Innovación y Universidades (MCIN/AEI/10.13039/501100011033) (Projects PID2023-147424NB-I00, PID2023-146849NB-I00, RED2022-134939-T and RED2022-134074-T, FPI predoctoral grant to C.C. and Margarita Salas grant (NextGenerationEU) to A.A.), from the Generalitat de

Catalunya (Project 2021-SGR-623) and from the European Union's Framework Programme for Research and Innovation Horizon Europe under the Marie Skłodowska-Curie Grant Agreement No. 101106492 (project title: Full-Fission). We would like to thank Dr. Pedro Salvador his help and support in the interpretation of EOS analysis.

References


- [1] a) E. Castro, A. H. Garcia, G. Zavala, L. Echegoyen, *J. Mater. Chem. B* **2017**, *5*, 6523–6535; b) T. Da Ros, in *Medicinal Chemistry and Pharmacological Potential of Fullerenes and Carbon Nanotubes* (Eds: F. Cataldo, T. Da Ros), Springer Netherlands: Dordrecht **2008**, pp. 1–21; c) N. Panwar, A. M. Soehartono, K. K. Chan, S. Zeng, G. Xu, J. Qu, P. Coquet, K. T. Yong, X. Chen, *Chem. Rev.* **2019**, *119*, 9559–9656; d) J. Ramos-Soriano, J. J. Reina, B. M. Illescas, N. de la Cruz, L. Rodríguez-Pérez, F. Lasala, J. Rojo, R. Delgado, N. Martín, *J. Am. Chem. Soc.* **2019**, *141*, 15403–15412.
- [2] a) A. Montellano López, A. Mateo-Alonso, M. Prato, *J. Mater. Chem.* **2011**, *21*, 1305–1318; b) D. Canevet, E. M. Pérez, N. Martín, *Angew. Chem. Int. Ed.* **2011**, *50*, 9248–9259.
- [3] a) S. Collavini, J. L. Delgado, *Sustain. Energy Fuels* **2018**, *2*, 2480–2493; b) L. Jia, M. Chen, S. Yang, *Mater. Chem. Front.* **2020**, *4*, 2256–2282; c) O. Fernandez-Delgado, P. S. Chandrasekhar, N. Cano-Sampaio, Z. C. Simon, A. R. Puente-Santiago, F. Liu, E. Castro, L. Echegoyen, *J. Mat. Chem. C.* **2021**, *9*, 10759–10767; d) M. Izquierdo, B. Platzer, A. J. Stasyuk, O. A. Stasyuk, A. A. Voityuk, S. Cuesta, M. Solà, D. M. Guldi, N. Martín, *Angew. Chem. Int. Ed.* **2019**, *58*, 6932–6937.
- [4] a) W. Śliwa, *Fullerene Sci. Technol.* **1995**, *3*, 243–281; b) A. Artigas, C. Castanyer, A. Roglans, A. Pla-Quintana, *Adv. Organomet. Chem.* **2024**, *82*, 135–189; c) I. Fernández, M. Solà, F. M. Bickelhaupt, *Chem. Eur. J.* **2013**, *19*, 7416–7422.
- [5] R. Taylor, *C. R. Chim.* **2006**, *9*, 982–1000.
- [6] a) N. Martín, J. L. Segura, F. Wudl, in *Fullerenes: From Synthesis to Optoelectronic Properties Developments in Fullerene Science* (Eds: D. M. Guldi, N. Martín) Springer, Dordrecht, **2002**, pp. 81–120; b) A. Hirsch, I. Lamparth, T. Grosser, *J. Am. Chem. Soc.* **1994**, *116*, 9385–9386; c) R. Schwenninger, T. Müller, B. Krautler, *J. Am. Chem. Soc.* **1997**, *119*, 9317–9318; d) G. Pareras, S. Simon, A. Poater, M. Solà, *J. Org. Chem.* **2022**, *87*, 5149–5157.
- [7] H. Hopf, M. S. Sherburn, *Synthesis* **2022**, *54*, 864–886.
- [8] For selected reviews, see: a) K. M. Brummond, J. E. DeForrest, *Synthesis* **2007**, *6*, 795–818; b) J. Ye, S. Ma, *Org. Chem. Front.* **2014**, *1*, 1210–1224; c) R. K. Neff, D. E. Frantz, *ACS Catal.* **2014**, *4*, 519–528; d) W.-D. Chu, Y. Zhang, J. Wang, *Catal. Sci. Technol.* **2017**, *7*, 4570–4579.
- [9] Selected reviews for the cycloisomerization of enynes, allenynes, allenenes and bisallenenes: a) B. M. Trost, M. J. Krische, *Synlett* **1998**, *1*, 1–16; b) C. Aubert, O. Buisine, M. Malacria, *Chem. Rev.* **2002**, *102*, 813–834; c) G. C. Lloyd-Jones, *Org. Biomol. Chem.* **2003**, *1*, 215–236; d) L. Zhang, J. Sun, S. A. Kozmin, *Adv. Synth. Catal.* **2006**, *348*, 2271–2296; e) V. Michelet, P. Y. Toullec, J.-P. Genêt, *Angew. Chem. Int. Ed.* **2008**, *47*, 4268–4315; f) E. Jiménez-Núñez, A. M. Echavarren, *Chem. Rev.* **2008**, *108*, 3326–3350; g) I. D. G. Watson, F. D. Toste, *Chem. Sci.* **2012**, *3*, 2899–2919; h) Y. Hu, M. Bai, Y. Yang, Q. Zhou, *Org. Chem. Front.* **2017**, *4*, 2256–2275; i) J.-X. Liu, S.-Q. Xu, Y.-P. Han, Y.-M. Liang, *Adv. Synth. Catal.* **2024**, *366*, 1220–1268; j) C. Aubert, L. Fensterbank, P. Garcia, M. Malacria, A. Simonneau, *Chem. Rev.* **2011**, *111*, 1954–1993; k) R. Zriba, V. Gandon, C. Aubert, L. Fensterbank, M. Malacria, *Chem. Eur. J.* **2008**, *14*, 1482–1491; l) B. Alcaide, P. Almendros, C. Aragoncillo, *Chem. Soc. Rev.* **2014**, *43*, 3106–3135; m) G. Chen, X. Jiang, C. Fu, S. Ma, *Chem. Lett.* **2010**, *39*, 78–81.
- [10] C. Castanyer, A. Artigas, N. Insa-Carreras, M. Solà, A. Pla-Quintana, A. Roglans, *Adv. Synth. Catal.* **2024**, *366*, 862–869.
- [11] a) A. Artigas, C. Castanyer, N. Roig, A. Lledó, M. Solà, A. Pla-Quintana, A. Roglans, *Adv. Synth. Catal.* **2021**, *363*, 3835–3844. For a similar process using alkenes instead of C60 as dienophiles, see: b) A. Artigas, J. Vila, A. Lledó, M. Solà, A. Pla-Quintana, A. Roglans, *Org. Lett.* **2019**, *21*, 6608–6613; c) J. Vila, M. Solà, A. Pla-Quintana, A. Roglans, *J. Org. Chem.* **2022**, *87*, 5279–5286.
- [12] D. Llerena, C. Aubert, M. Malacria, *Tetrahedron Lett.* **1996**, *37*, 7027–7030.
- [13] Selected recent examples with several metals: a) Y. Oonishi, Y. Kitano, Y. Sato, *Angew. Chem. Int. Ed.* **2012**, *51*, 7305–7308; b) X. Deng, L.-Y. Shi, J. Lan, Y.-Q. Guan, X. Zhang, H. Lv, L. W. Chung, X. Zhang, *Nat. Commun.* **2019**, *10*, 949; c) F. Jaroschik, A. Simonneau, G. Lemièrre, K. Cariou, N. Agenet, H. Amouri, C. Aubert, J.-P. Goddard, D. Lesage, M. Malacria, Y. Gimbert, V. Gandon, L. Fensterbank, *ACS Catal.* **2016**, *6*, 5146–5160; d) K.-F. Wei, Q. Liu, G. Ma, X.-L. Jiang, X.-H. Zhu, G.-X. Ru, W.-B. Shen, *Commun. Chem.* **2023**, *6*, 104; e) J. C. Nieto-Carmona, I. Manjón-Mata, M. T. Quirós, G. Caballero-Santiago, F. Pérez-Maseda, D. J. Cárdenas, *Adv. Synth. Catal.* **2024**, *366*, 790–797.
- [14] N. Cadran, K. Cariou, G. Hervé, C. Aubert, L. Fensterbank, M. Malacria, J. Marco-Contelles, *J. Am. Chem. Soc.* **2004**, *126*, 3408–3409.
- [15] E. Soriano, J. Marco-Contelles, *Chem. Eur. J.* **2005**, *11*, 521–533.
- [16] Y. Zhou, A. Nikbakht, F. Bauer, B. Breit, *Chem. Sci.* **2019**, *10*, 4805–4810.
- [17] P. Vermeeren, M. Dalla Tiezza, M. E. Wolf, M. E. Lahm, W. D. Allen, H. F. Schaefer III, T. A. Hamlin, F. M. Bickelhaupt, *Phys. Chem. Chem. Phys.* **2022**, *24*, 18028–18042.
- [18] Z. Yu, M. Shi, Y. Wei, *Molecules* **2024**, *29*, 1085.
- [19] I. González, A. Pla-Quintana, A. Roglans, A. Dachs, M. Solà, T. Parella, J. Farjas, P. Roura, V. Lloveras, J. Vidal, *Chem. Commun.* **2010**, *46*, 2944–2946.

- [20] S. Vásquez-Céspedes, X. Wang, F. Glorius, *ACS Catal.* **2018**, *8*, 242–257.
- [21] a) V. Postils, C. Delgado-Alonso, J. M. Luis, P. Salvador, *Angew. Chem. Int. Ed.* **2018**, *57*, 10525–10529; b) M. Gimferrer, A. Aldossary, P. Salvador, M. Head-Gordon, *J. Chem. Theory Comput.* **2022**, *18*, 309–322.
- [22] M. J. Frisch, G. W. Trucks, H. B. Schlegel, G. E. Scuseria, M. A. Robb, J. R. Cheeseman, G. Scalmani, V. Barone, G. A. Petersson, H. Nakatsuji, X. Li, M. Caricato, A. V. Marenich, J. Bloino, B. G. Janesko, R. Gomperts, B. Mennucci, H. P. Hratchian, J. V. Ortiz, A. F. Izmaylov, J. L. Sonnenberg, D. Williams-Young, F. Ding, F. Lipparini, F. Egidi, J. Goings, B. Peng, A. Petrone, T. Henderson, D. Ranasinghe, V. G. Zakrzewski, J. Gao, N. Rega, G. Zheng, W. Liang, M. Hada, M. Ehara, K. Toyota, R. Fukuda, J. Hasegawa, M. Ishida, T. Nakajima, Y. Honda, O. Kitao, H. Nakai, T. Vreven, K. Throssell, Montgomery, J. A. , Jr., J. E. Peralta, F. Ogliaro, M. J. Bearpark, J. J. Heyd, E. N. Brothers, K. N. Kudin, V. N. Staroverov, T. A. Keith, R. Kobayashi, J. Normand, K. Raghavachari, A. P. Rendell, J. C. Burant, S. S. Iyengar, J. Tomasi, M. Cossi, J. M. Millam, M. Klene, C. Adamo, R. Cammi, J. W. Ochterski, R. L. Martin, K. Morokuma, O. Farkas, J. B. Foresman, D. J. Fox, *Gaussian 16, Revision C.01*, Gaussian, Inc., Wallingford CT **2016**.
- [23] a) A. D. Becke, *J. Chem. Phys.* **1993**, *98*, 5648–5652; b) C. Lee, W. Yang, R. G. Parr, *Phys. Rev. B* **1988**, *37*, 785–789.
- [24] a) T. H. Dunning, *J. Chem. Phys.* **1989**, *90*, 1007–1023; b) D. E. Woon, T. H. Dunning, *J. Chem. Phys.* **1993**, *98*, 1358–1371.
- [25] K. A. Peterson, D. Figgen, M. Dolg, H. Stoll, *J. Chem. Phys.* **2007**, *126*, 124101.
- [26] R. E. Stratmann, J. C. Burant, G. E. Scuseria, M. J. Frisch, *J. Chem. Phys.* **1997**, *106*, 10175–10183.
- [27] A. V. Marenich, C. J. Cramer, D. G. Truhlar, *J. Phys. Chem. B* **2009**, *113*, 6378–6396.
- [28] S. Grimme, J. Antony, S. Ehrlich, H. A. Krieg, *J. Chem. Phys.* **2010**, *132*, 154104.
- [29] P. Atkins, J. De Paula, *The Elements of Physical Chemistry*, 3rd ed, Oxford University Press, Oxford **2006**.
- [30] M. Álvarez-Moreno, C. de Graaf, N. López, F. Maseras, J. M. Poblet, C. Bo, *J. Chem. Inf. Model.* **2015**, *55*, 95–103.

RESEARCH ARTICLE

On the Functionalization of C_{60} with Vinylallenes Generated *in situ* by Rhodium Catalysis

Adv. Synth. Catal. **2024**, *366*, 1–11

 C. Castanyer, A. Artigas, M. Solà, A. Pla-Quintana*, A. Roglans*

